

EFFECT OF DIFFERENT STAGES OF TENSILE DEFORMATION ON MAGNETIC BARKHAUSEN EMISSION IN HIGH STRENGTH LOW ALLOY STEEL

S. Vaidyanathan, V. Moorthy, P. Kalyanasundaram, T. Jayakumar,
and Baldev Raj
Metallurgy and Materials Group
Indira Gandhi Centre for Atomic Research
Kalpakkam- 603 102, INDIA

INTRODUCTION

Micromagnetic techniques have been considered as a potential non-destructive evaluation (NDE) method for microstructural characterization and stress/strain measurements in ferritic steels [1-14]. The effect of tensile deformation on micromagnetic parameters has been studied by many researchers [8-14]. Most of these studies have been done only in the elastic region and the obtained relation between magnetic parameters and the applied stress has been used to determine the residual stresses, considering that the residual stress level will not exceed the yield stress of the material. These studies have not taken into account the microstructural changes due to dislocations generation by the plastic deformation.

The progressive deformation can be classified into different stages such as perfectly elastic, micro-plastic yielding, macro-yielding and progressive plastic deformation. The magnetization process would vary to different extent in these four stages depending on the effect of applied or residual stresses and the dislocation density. In order to understand this, the influence of uniaxial tensile deformation on MBE parameters has been studied in a high strength low alloy (HSLA) steel in both stressed and unstressed conditions.

EXPERIMENTAL PROCEDURE

The chemical composition of the low alloy steel used in this study is given in Table I. The plain and the composite tensile samples with 6 mm thickness, 20 mm width and 60 mm gauge length were fabricated as per the ASTM standards E-8 from the as received base plate and from the weld pad respectively. The composite specimens having weld, heat affected zone (HAZ) and base regions were fabricated in a such a way that the weld lies at the centre of specimen length and perpendicular to the stress direction.

Table I: Chemical composition (wt.%) of the low alloy steel.

Steel	Cr	Mo	Mn	C	P	Si	S	Ni	Cu	Fe
Low alloy steel	0.32	0.28	0.24	0.11	0.008	0.23	0.012	2.1	0.5	Balance

A block diagram of the experimental set-up for the measurement of magnetic parameters is shown in Fig. 1. The samples were subjected to continuously varying cyclic magnetic field with magnetizing frequencies of 0.1 and 50 Hz in an electromagnetic yoke. The current applied to the yoke has been calibrated with respect to the magnetic field. The samples were subjected to a maximum tangential magnetic field of ± 12000 A/m. The tangential magnetic field has been measured on the sample surface using a Hall probe connected to a Gaussmeter (MG-50 Walker Scientific Inc). The MBE signal was acquired by a 1 mm diameter ferrite cored surface probe having 4000 turns. The surface MBE probe has been used to scan the weld, HAZ and base metal regions in the composite weldment specimens. At 50 Hz excitation, the MBE signal was amplified to 60 dB using a low noise filter amplifier (Stanford) with 10kHz - 1MHz bandwidth and Philips RMS voltmeter. At 0.1 Hz excitation, the profile of the RMS voltage of the MBE signal and the hysteresis loop were measured using a PC based data acquisition system.

The samples were subjected to room temperature uniaxial tensile test at a nominal strain rate of 2.8×10^{-4} /s in an universal testing machine (INSTRON 1195). The samples were loaded to different stress levels and the MBE measurements were made on-line at 50 Hz excitation in both stressed and unstressed conditions. The hysteresis loop and the profile of the RMS voltage of the MBE were measured at 0.1Hz only after unloading from each stress level. The measurements were repeated upto ultimate tensile stress.

RESULTS AND DISCUSSION

Figures 2(a-b) show the typical variation in the RMS voltage profile of the MBE (at 0.1Hz excitation) as a function of the current applied to the yoke in the unstressed condition for different prior applied stress levels in the base metal specimen. Figure 3 shows the variation in the MBE level (at 50 Hz excitation) in the loaded and unloaded conditions and the applied stress as a function of % nominal strain for two base metal specimens. Figure 4 shows the same for a typical composite weldment specimen at weld, HAZ and base metal regions. The behaviour of the MBE at both excitations remains same. Also, the plain specimen and the different regions in the composite weldment specimen show similar behaviour in the MBE with strain in both loaded as well as unloaded conditions (Fig. 3 and 4). The difference in the MBE level at the weld, HAZ and base metal regions in the composite specimen (Fig. 4) is attributed to the microstructural variations in these regions. It has been shown earlier by the authors that, in Cr-Mo steel weldments, even after the post-weld heat treatment

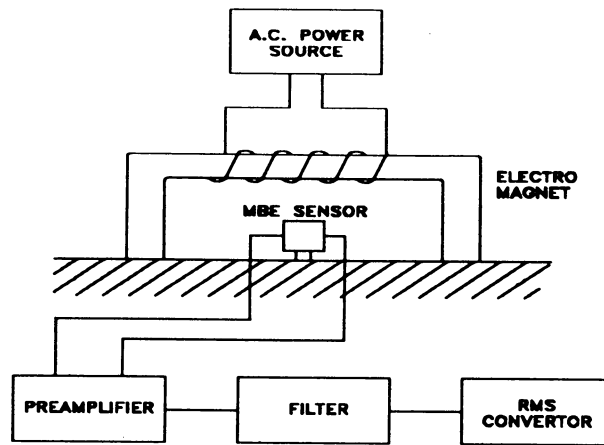


Fig. 1. Block diagram of the experimental set-up.

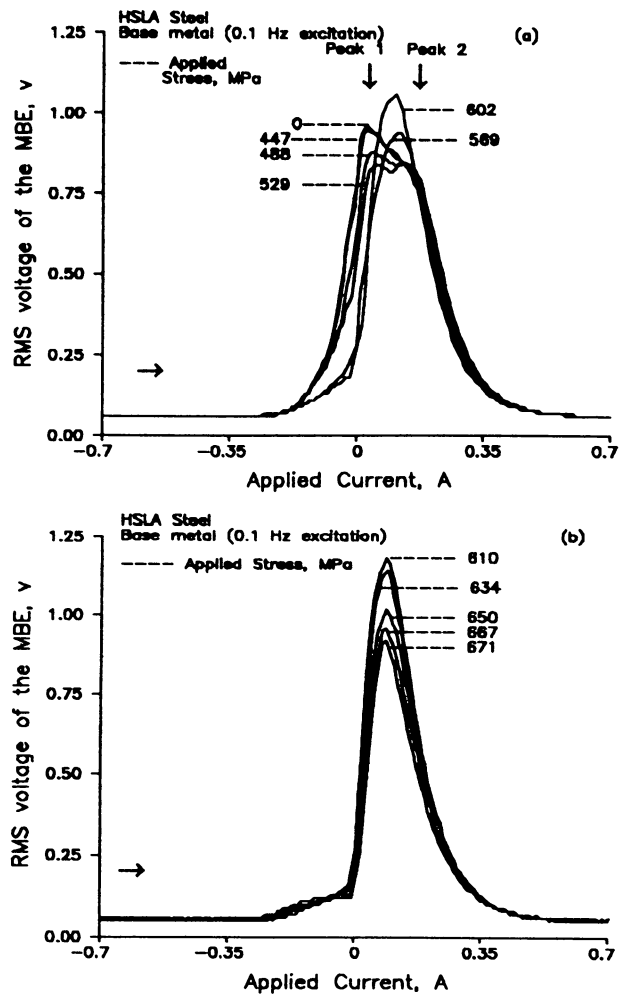


Fig. 2. Typical variation in the RMS voltage profile of the MBE as a function of the current applied to the yoke for base metal specimen after unloading the specimen from different prior stress levels.

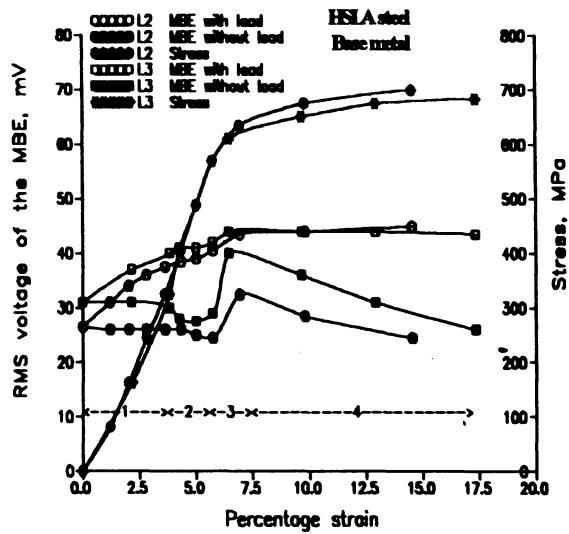


Fig. 3. Variation in the MBE level in the loaded and unloaded conditions and the applied stress as a function of % nominal strain for two base metal specimens.

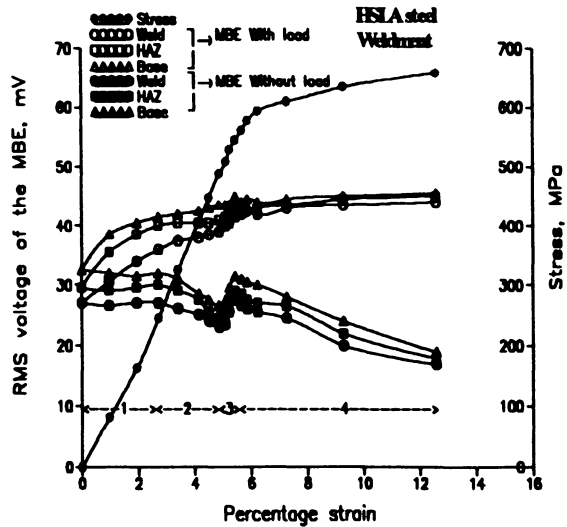


Fig. 4. Typical variation in the MBE level in the loaded and unloaded conditions and the applied stress as a function of % nominal strain at weld, HAZ and base metal regions for composite specimen.

(PWHT), the MBE, the microstructure and the hardness varies significantly in these regions [15]. The weld region shows the highest hardness, followed by HAZ and base metal regions. The MBE level was lowest at the weld and it increased with the distance from the weld [15]. The present study also shows similar variations in the MBE level at different regions in the weldment irrespective of the prior stress level.

The variation in the MBE level with strain can be divided into four stages such as (1) perfectly elastic, (2) microplastic yielding, (3) macro-yielding (4) progressive plastic deformation as indicated in Figs. 3 and 4. The RMS voltage profile of the MBE also shows the distinct changes at different stages of deformation (Figs. 2(a-b)). The RMS voltage profile of the MBE for the virgin sample shows sharp slope changes indicating the possibility of splitting into two peaks (peak 1 and peak 2 in Fig. 2(a)). The authors have shown earlier [5-7], such sharp slope changes in short tempered carbon steel and Cr-Mo steel which on subsequent tempering develops into two clear peaks. This has been explained based on the two stage magnetization process in tempered ferritic steels [5-7]. The peak 1 has been attributed to the domain wall movement overcoming the grain boundary resistance and the peak 2 has been attributed to the domain wall movement overcoming the second phase precipitates.

EFFECT OF PRE-YIELD AND POST-YIELD DEFORMATION ON MBE

Perfectly Elastic - Stage 1

Figure 5 shows the typical variation in the MBE level in the loaded and unloaded conditions with strain during stage 1 deformation for a base metal. It can be observed that, during the initial stages of elastic loading (stage 1), the MBE increases linearly with strain in the loaded condition and remains same as that in the virgin condition when it is measured in the unloaded condition. The increase in the MBE in the stressed condition shows the effect of applied tensile stress on the domain realignment along the stress direction. The unaffected MBE level in the unloaded condition shows the perfectly elastic deformation. The RMS voltage profile of the MBE also shows no significant changes upto 447 MPa (Fig. 2(a)). This confirms the unaltered microstructure after unloading in this region. In this elastic region, the value of the applied stress can be determined from the change in the MBE level (linear relationship between the MBE and the applied stress).

Micro-plastic Yielding - Stage 2

Figure 6 shows the typical variation in the MBE level in the loaded and unloaded conditions with strain during stage 2 deformation for a base metal. Well below the macroyielding (about 50% of the yield stress), the MBE level starts decreasing significantly. This can be identified from region 2 of the Fig. 3 and Fig. 6, by the decrease in the slope of the MBE vs. strain plot in the loaded condition and the decrease in the MBE level in the unloaded condition. This is also evident from the decrease in the peak 1 height of the MBE profile (Fig. 2(a)). This is attributed to the microplastic yielding by the operation of Frank-Read and grain boundary dislocation sources creating dislocation pile-ups which reduce the mean free path of the domain wall displacement. It is well known that the grain boundary is one of the major source of dislocation generation apart from the Frank-Read type sources. These dislocation

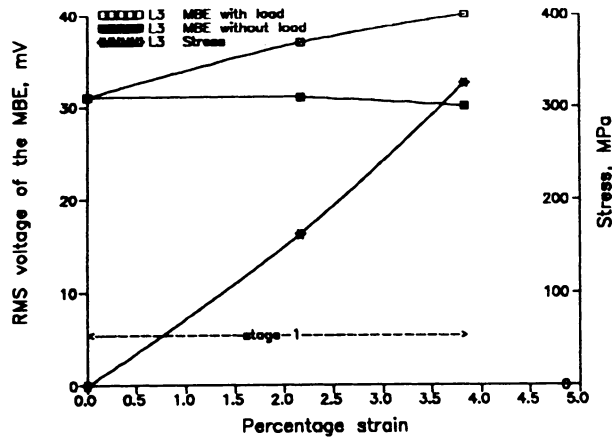


Fig. 5. Typical variation in the MBE level in the loaded and unloaded conditions and the applied stress as a function of % nominal strain during stage 1 deformation in base metal.

sources would start operating even during the macroelastic region (about 50% of the yield stress) causing the microplastic yielding. The dislocation pile ups generated within the grains during micro-yielding would reduce the mean free path of domain wall displacement. This results in the net reduction in the MBE level in the loaded condition in spite of the presence of tensile stress which would tend to increase the MBE by the stress induced domain alignments. This is reflected by the decrease in the slope MBE vs. strain plot in the loaded condition (stage 2 in Fig. 3) and the decrease in the peak 1 height in the MBE profile (Fig. 2(a)). The effect of microplastic yielding is well reflected by the decrease in the MBE level in the unloaded condition. In this micro-yield region, the changes in the MBE level in the unloaded condition show effect of only dislocations. When this difference in MBE is subtracted from the MBE level in the loaded condition, the contribution from the applied stress alone can be determined in this stage 2 also.

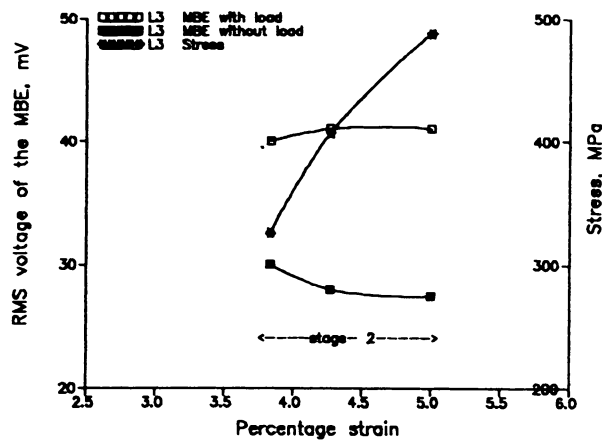


Fig. 6. Typical variation in the MBE level in the loaded and unloaded conditions and the applied stress as a function of % nominal strain during stage 2 deformation in base metal.

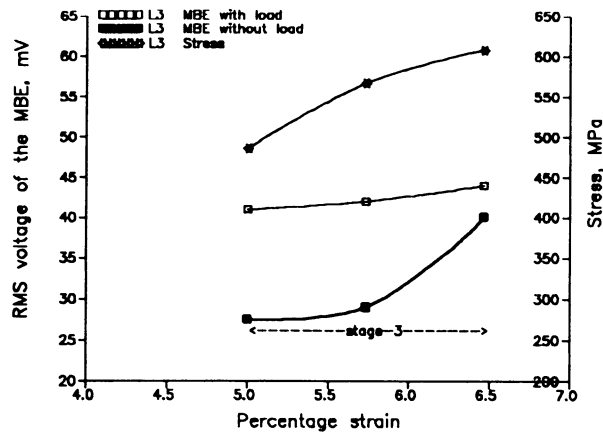


Fig. 7. Typical variation in the MBE level in the loaded and unloaded conditions and the applied stress as a function of % nominal strain during stage 3 deformation in base metal.

Macro-Yielding - Stage 3

Figure 7 shows the typical variation in the MBE level in the loaded and unloaded conditions with strain during stage 3 deformation for a base metal. It can be observed from region 3 of the Fig. 3 and Fig. 7 that, there is a sudden rise in the MBE level corresponding to the yield stress in both loaded and unloaded conditions. The two peaks in the MBE profile merges into a single central peak and the central peak height increases rapidly near the macro-yielding (Fig. 2(a-b)). It is well known that the grain rotation occurs at the yield stress in order to accommodate the differential strain generated at the grain boundary to maintain the grain boundary integrity for compatible deformation. The grain rotation would result in the alignment of the magnetic domains nearest to the stress direction and would contribute to the sudden rise in the MBE level. The increase in the MBE level in stage 3 is more pronounced in the unloaded condition than that in the loaded condition. This is because of the fact that, the domain alignment from the grain rotation phenomenon would reduce the contribution of the

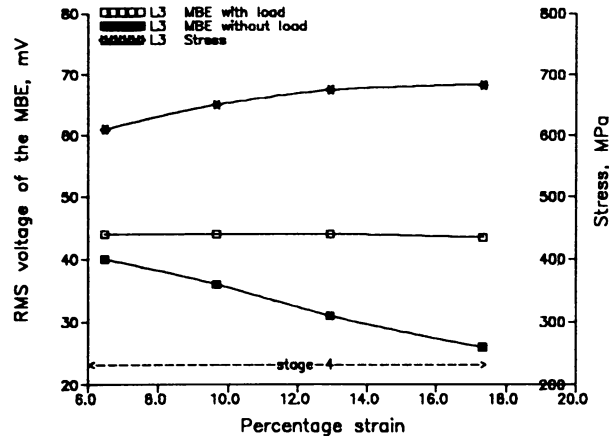


Fig. 8. Typical variation in the MBE level in the loaded and unloaded conditions and the applied stress as a function of % nominal strain during stage 4 deformation in base metal.

stress induced domain alignment in the case of stressed condition. Still, this is reflected by the increase in the slope of the MBE vs. strain plot in the stressed condition (region 3 of Fig. 3).

Progressive Plastic Deformation - Stage 4

Figure 8 shows the typical variation in the MBE level in the loaded and unloaded conditions with strain during stage 4 deformation for a base metal. With progressive deformation, it can be observed from region 4 of the Fig. 3 and Fig. 8 that the MBE level remains more or less constant in the loaded condition and decreases more or less linearly with strain in the unloaded condition. The central peak height in the MBE profile also decrease with strain (Fig. 2(b)). The constant behaviour of MBE in the loaded condition can be attributed to the balancing contributions from two opposing effects of the applied tensile stress and the increase in the dislocation density. It is already mentioned that the tensile stress would enhance the MBE level. The applied tensile stress would align the domains along the stress direction and would tend to nullify the effect of the dislocations. Hence, in the loaded condition, the effect of increasing dislocation density is not reflected in the MBE level.

It is expected that the variations in the stress state of surface (biaxial-plane stress) and the bulk (triaxial-plane strain) would cause the difference in the deformation behaviour of the surface and bulk of the sample. Earlier studies [10,11] showed that the tensile deformation introduces residual compressive stress near the surface layers. With progressive plastic deformation, it is considered that, in the surface region, the magnetization process is affected both by the residual compressive stress and the increase in the dislocation density. Hence, the linear decrease in the MBE in the unloaded condition is attributed to the combined effect of increase in the dislocation density and the residual compressive stress.

CONCLUSION

This study shows that the MBE technique can be used to identify the different stages of deformation such as perfectly elastic, microplastic yielding, the macro-yielding and progressive plastic deformation in ferritic steel base and weldments. Within the elastic region (stage 1), the applied stress can be determined from the change in the MBE level. It is clearly shown in this study that, dislocation generation even during micro-plastic yielding (stage 2) affect the MBE level significantly. The macro-yield phenomenon (stage 3) is reflected by the sharp increase in the MBE level. With progressive plastic deformation (stage 4), the MBE decreases in a linear manner. The difference in the MBE level with and without the applied stress shows the combined effect of the dislocation density and the applied / residual stress. For residual stress determination using the MBE technique, the effect of dislocation density should be taken into account. With prior calibration by X-ray diffraction measurement at different stages of deformation, the MBE can be related to the residual stress generated at different strain level. Since, the MBE measurement system can be made portable, it can be considered as simple, versatile technique and easily applicable in the field for residual stress measurements.

ACKNOWLEDGMENT

Authors are thankful to Dr. Placid Rodriguez, Director, Indira Gandhi Centre for Atomic Research, Kalpakkam for his constant encouragement and support during this study.

REFERENCES

1. S. Tiitto, *Acta Polytechnica Scandinavica, Appl.Phy.Series*, 1977, vol. 119, pp. 1-80.
2. D.J. Buttle, C.B. Scruby, J.P. Jakubovics, and G.A.D. Briggs, *Phil. Mag., A*, 1987, vol. 55A (6) pp.717-734.
3. C. Gatelier-rothca, P. Fleischmann, J. Chicois, and R. Fougeres, *Nondestr. Test. Eval.*, 1992, vol. 8-9, pp. 591-602.
4. J. Kameda, and R. Ranjan, *Acta metall.*, 1987, vol. 35 (7) pp.1515-1526.
5. V.Moorthy, S. Vaidyanathan, T. Jayakumar and Baldev Raj, *J. Magnetism and Magnetic Mater.*, 1997, vol. 171, pp. 179-189.
6. Baldev Raj, V.Moorthy and S.Vaidyanathan, *Materials Evaluation*, 1997, vol. 55 (1) pp. 81-84.
7. V.Moorthy, S. Vaidyanathan, T. Jayakumar and Baldev Raj, *Phil. Mag. A* , 1998, vol. 77 (6) pp. 1499-1514 (1998).
8. D.J. Buttle, C.B. Scruby, G.A.D. Briggs, and J. Jakubovics, *Proc. R. Soc. Lond*, 1987, vol. 414A, pp. 469-497.
9. R. Rautioaho, L. P. Karjalainen, and M. Moilanen, *J.Magnetism and Magnetic Materials*, 1988, vol. 73, pp. 96-102.
10. L.P. Karjalainen, and M. Moilanen, *NDT Int.*, 1979, vol. 12 (2) pp. 51-55.
11. R. Langman, *NDT Int.*, 1987, vol. 20 (2) pp. 93-99.
12. A.K. Sengupta and W.A. Theiner, *Mater. Evaluation*, 1995, vol. 53 (5) pp. 554-561.
13. S.M. Thompson and B.K. Tanner, *J. Magnetism and Magnetic Mater.*, 1994, vol. 132, pp. 71-88.
14. D.C. Jiles, *J. Phys. D.*, 1988, vol. 21, pp. 1196-1204.
15. V. Moorthy, S.Vaidyanathan, K. Laha, T. Jayakumar, K. Bhanu Sankara rao and Baldev Raj, *Mater. Sci. Engg.*, 1997, vol. 231A, pp. 98-104.